Adaptive Robust Control Systems in KAGRA Vibration Isolation Systems

Tsang Terrence Tak Lun

November 20, 2019

1 Preface

This document was entitled "Adaptive Control Systesm for Preisolator Stages in KAGRA Vibration Isolation Systems" before I changed it to the current one. I made this change because, in the middle of all this, I realized adaptive + robust control can be part of something much greater and potentially becomes the ultimate solution for all suspension problems in KAGRA where payload control systems were continuously being tweaked to prevent modes from ringing up during the lock-acquisition. The idea of adaptive robust control system is to have an adaptive control system that can automatically change the controller gain according to real-time seismic noise level so the total quadrature sum of the seismic noise and sensor noise can be minimized. This document will begin by defining the control problem for preisolator and later we will show that the idea can be generalized for all stages in a multiple pendulum suspension.

2 Abstract

We proposed an adaptive robust control scheme to actively suppress ground disturbance to the preisolator platform. Robust controller synthesis method allows guaranteed stability and can be automatically done given a modeled system. Adaptive control method allows the control gain to be automatically tuned high if strong suppression is needed while the control gain is automatically tuned low to avoid excess noise inject when disturbance rejection is not important. This facilitates stable interferometer and quiet observation as a result. To further enhance the performance of the controller, a global optimization step is also proposed during the self-tuning process of the adaptive controller. The use of adaptive filter and least mean square algorithm is also proposed as sensor correction filter, feedforward filter, cross-coupling decoupling filter and a tool for accurate system identification.

(Not written yet) Adaptive control requires real-time optimization and can be computationally costly. Online optimization also requires non-negligible time window which reduces the efficiency of the adaptive control approach. Because the optimization process is simply an input-output process, machine learning algorithms such as deep neural network can be used to replace the controller optimization and synthesis process. In this way, the time required for long optimization can be drastically reduced hence enhancing the efficacy of the adaptive approach.

3 Background

After the implementation of sensor correction for the relative sensors at the pre-isolator(PI)/inverted pendulum(IP) stages, a question raised: is additional loop gain needed at micro-seismic frequencies? Without sensor correction, the control bandwidth at the IP stage was limited at the first resonance which is located at frequency lower than the micro-seismic frequencies, meaning that the overall loop gain was very loop except at very low frequencies. This

is to prevent the control system from introducing low-frequency seismic noise which was coupled to the relative sensors. Now that correction is implemented, the corrected sensor signal is free from seismic noise.

One would argue that the control bandwidth can be extended so seismic noise can be further suppressed. However, this statement is not absolutely true because the optimal loop gain ultimately depends on both the seismic noise and the sensor noise. Having too much control gain would introduce additional sensor noise while having insufficient attenuation would make the system susceptible to ground disturbances. Therefore, instead of blindly increasing the loop gain, one has to properly design the optimal controller according to the sensor noise and the ground noise.

Moreover, the seismic noise level is not static. In fact, the ground motion in KAGRA varies drastically depending on natural events such as typhoon and earthquakes. Therefore, it can be seen that the ground noise level is a actually time-varying quantity. This would mean that a static controller is not always optimal. This is where adaptive control comes into play. We propose a form of adaptive control system which has loop-gain continuously optimized according to real-time measurement of ground motion. In laymen terms, when the ground disturbance is high, a higher controller gain should be high for seismic noise rejection. But, when the seismic noise is low, the gain is lowered so control noise is lower in favour of observation. In this document, we will discuss how the strategy can be achieved.

4 Controller design

4.1 Definition

We are aware that definitions in quantities in a control system can be different between that from gravitational wave physics and that from control engineering. Therefore, for this particular discussion, it is important to establish a common definition here to prevent confusion and misunderstanding. Throughout the discussion, we focus on the preisolator translational degrees of freedom unless otherwise specified. A similar analysis can be applied to other degrees of freedom but this is not in the scope of this particular discussion.

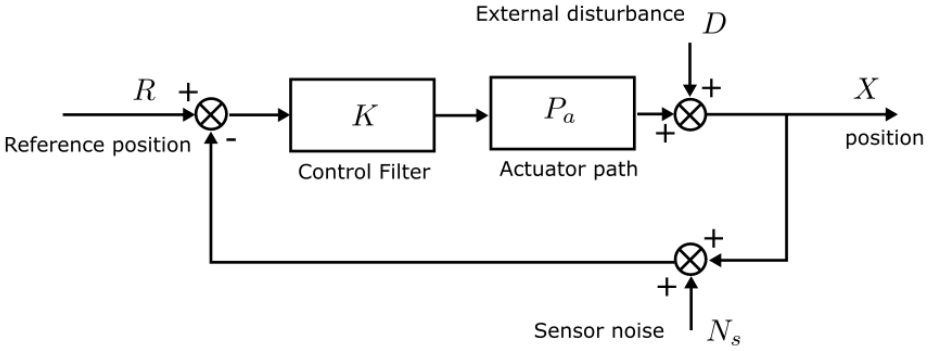

Figure 1: A block diagram representing the feedback system of the preisolator.

For a preliminary analysis, we consider a feedback system with a static reference input, external disturbance and sensor noise. A block diagram analogy is shown in Fig. 1. The loop gain/loop transfer function is P_aK, where P_a is the actuator to displacement transfer function. The reference input R plays almost no roles in the controller optimization process but its existence add an additional requirement for the controller K which has to have infinite gain at DC. External disturbances are referred to exogenous inputs that directly affects the plant output. A typical example would be the gound motion X_g which couples to the preisolator platform via the harmonic oscillator-like inverted pendulum path P_{IP}. In fact, the gound disturbance $D = P_{IP}X_g$ is the only significant disturbance in our case, but we shall keep using the term disturbance or D without loss of generality. At last, the sensor noise N_s refers to any additional uncertainties contaminating the measurement of the plant output X (i.e. the position). In this case, the total sensor noise would contain intrinsic noise from the relative displacement sensor (LVDT) N_{LVDT} and the intrinsic noise from seismometer N_{seis}, i.e. $N_s = N_{LVDT} + C_{sc}N_{seis}$, where C_{sc} is the sensor correction filter (assumed to be unity for simplicity). Expressing the preisolator position in terms of the exogenous inputs, we

get

$$X = \left(\frac{P_a K}{1 + P_a K}\right) R + \left(\frac{1}{1 + P_a K}\right) D - \left(\frac{P_a K}{1 + P_a K}\right) N_s, \tag{1}$$

note that all variables and functions are expressed in the frequency domain.

4.2 Goal

As is standard in classical control systems, the objective of the feedback controller design is to find a stabilizing controller K such that certain performance goals can be reached. For long-term stability of the main interferometer, the preisolator should be held relatively still at reference position for preserving the alignment of suspended optic. Also, the residual motion of the preisolator platform due to external disturbances should be minimized while having acceptable attenuated sensor noise level introduced to the system.

To fix the preisolator DC position to a reference value, the controller has to have very high gain at DC and very low frequencies. This part of the design is mostly trivial and can be static. This is usually handled by an fixed-gain integrator. At other higher frequencies, the design becomes not trivial because there exists an optimal gain at each frequency that would minimize the residual motion of the preisolator stage. At non-zero frequencies, R vanishes and the displacement of the preisolator reads

$$X\left(f > 0\right) = \left(\frac{1}{1 + P_a K}\right) D - \left(\frac{P_a K}{1 + P_a K}\right) N_s, \tag{2}$$

where it only depends on the ground motion disturbance and the sensor noise. To minimize residual motion, the coupling attenuation terms should be minimized. The attenuation of the external disturbance and sensor noise are $S \equiv \left(\frac{1}{1+P_a K}\right)$ and $T \equiv \left(\frac{P_a K}{1+P_a K}\right)$ respectively.[1] However, as can be shown algebraically, simultaneous minimization of S and T is impossible. This is because S and T are complementary to each other, meaning that when one is small, the other is close to unity.

$$S + T = \left(\frac{1}{1 + P_a K}\right) + \left(\frac{P_a K}{1 + P_a K}\right) = 1. \tag{3}$$

Therefore, the problem becomes finding an optimal controller K_{opt} such that the residual motion $\left\langle X^2 \right\rangle$ due to D and N_s is minimized.

4.2.1 Prove that K_{opt} Must Exist at $K \neq \infty$

At first glance, it would seem that having a high gain controller $K \to \infty$ is a universal solution to suppressing ground noise. However, having a high gain controller poses a few problems such as instability and process saturation. Therefore, it is not ideal vibration isolation systems in gravitational wave observatory which demands long-term stability and robustness. An alternative would be looking for an optimal gain that can achieve the same or better performance as the infinite gain controller. That said, as we will see later in this section, the optimal filter can be discrete in frequency space and therefore are not realistic. In this way, the design goal becomes to controller a causal controller that follows closely to the optimal one at frequencies where performance is critical.

Since the disturbance and sensor noise are assumed to be uncorrelated and that they are stochastic in nature, the time averaged residual displacement in power spectral density is expressed as the quadrature sum of the attenuated disturbances and noise,

$$\left\langle X^2 \right\rangle = \left|\frac{1}{1 + P_a K}\right|^2 \left\langle D^2 \right\rangle + \left|\frac{P_a K}{1 + P_a K}\right|^2 \left\langle N_s^2 \right\rangle. \tag{4}$$

By taking the derivative of $\left\langle X^2 \right\rangle$ with respect to K and set it to zero,

$$\frac{d}{dK} \left\langle X^2 \right\rangle = 0, \tag{5}$$

[1] Just a note here. In control theory, S and T are called the sensitivity function and the complementary sensitivity function respectively. They are useful quantities in robust control analysis. Further discussion not needed.

the critical points of $\langle X^2 \rangle$ as a function of K can be found at

$$K = K_{crit} = \frac{\langle D^2 \rangle}{\langle N_s^2 \rangle} \frac{1}{P_a}, \tag{6}$$

where $\frac{\langle D^2 \rangle}{\langle N_s^2 \rangle}$ happens to be some sort of SNR. At the critical point, the residual motion is

$$\langle X^2 \rangle_{crit} = \langle X^2 \rangle \Big|_{K=K_{crit}} = \frac{\langle N_s^2 \rangle^2 \langle D^2 \rangle + \langle D^2 \rangle^2 \langle N_s^2 \rangle}{\langle N_s^2 \rangle^2 + \langle D^2 \rangle^2 + 2 \langle N_s^2 \rangle \langle D^2 \rangle}. \tag{7}$$

To show that this critical point is a minimum, consider the case when $K = 0$ and $K \to \infty$,

$$\langle X^2 \rangle \Big|_{K=0} = \langle D^2 \rangle, \tag{8}$$

and

$$\langle X^2 \rangle \Big|_{K\to\infty} = \langle N_s^2 \rangle. \tag{9}$$

It can be seen that $\langle X^2 \rangle_{crit}$ is indeed the global minima because

$$\frac{\langle X^2 \rangle_{crit}}{\langle X^2 \rangle \Big|_{K=0}} = \frac{\langle N_s^2 \rangle^2 + \langle D^2 \rangle \langle N_s^2 \rangle}{\langle N_s^2 \rangle^2 + \langle D^2 \rangle^2 + 2 \langle N_s^2 \rangle \langle D^2 \rangle} \leq 1, \tag{10}$$

$$\frac{\langle X^2 \rangle_{crit}}{\langle X^2 \rangle \Big|_{K\to\infty}} = \frac{\langle N_s^2 \rangle \langle D^2 \rangle + \langle D^2 \rangle^2}{\langle N_s^2 \rangle^2 + \langle D^2 \rangle^2 + 2 \langle N_s^2 \rangle \langle D^2 \rangle} \leq 1, \tag{11}$$

and both $\langle D^2 \rangle$ and $\langle N_s^2 \rangle$ are positive definite. Therefore, the optimal control gain K_{opt} that minimizes the residual motion exists and is at exactly K_{crit} and the residual motion $\langle X^2 \rangle$ is ultimately limited at $\langle X^2 \rangle_{min} = \langle X^2 \rangle_{crit}$. Another purpose of this two comparison Eqn. 10 and Eqn. 11 is to show that the minimal residual motion that can be achieved

Unfortunately, this only works independently at each frequency points. Finding a continuous functional form of the optimal control gain $K_{opt}(f)$, or in the Laplace domain, $K_{opt}(s)$ would be almost impossible in this sense, since the power spectrum $\langle D^2 \rangle$ and $\langle N_s^2 \rangle$ are not guaranteed to be continuous and have no predetermined functional form. Another way to explain why it would be impossible to have such an optimal filter is to look at the loop transfer function $P_a K_{opt}$. Since K_{opt} is inversely proportional to P_a, the loop transfer function is effectively a zero-phase filter. And, it would be impossible to use a zero-phase filter as an online control filter because it is not casual, as in, the filter depends on future inputs to compute the present output.

Although it would seem that it is impossible to automatically generate optimal controllers using this approach, the theoretical optimal loop transfer function $P_a K_{opt}$ provides a very good hint how the actual loop transfer function should look like. Moreover, the theoretical minimal residual motion $\langle X^2 \rangle_{min}$ is also a reference for evaluating the performance of the controller. Therefore, the design objective becomes to construct a controller such that it is as close to K_{opt} as possible ,or to design a controller such that the designed residual $\langle X^2 \rangle$ is as close to $\langle X^2 \rangle_{min}$ as possible.

Example

As an example, we approximate the seismic noise as an integrator with a second order system with resonance frequency at 0.2 Hz and quality factor of 2.5 to mimic the micro-seismic noise. The seismic noise goes through the inverted pendulum path P_{IP} which is approximated as cP_a, where c is a constant such that the inverted pendulum has unity DC gain. The sensor noise spectrum is approximated as constant at higher frequencies with $1/f$ descent to mimic sensor noise of the seismometer. Here, we use the SR2 actuation path as an example. These quantities will continue to be used for further analysis unless otherwise specified. Fig. 2 shows the amplitude spectral density of the external disturbance D, the sensor noise N_s and the minimum of the residual motion. Fig. 3 shows the magnitude plot of the optimal gain K_{opt}, the actuation plant P_a and the loop gain $P_a K_{opt}$.

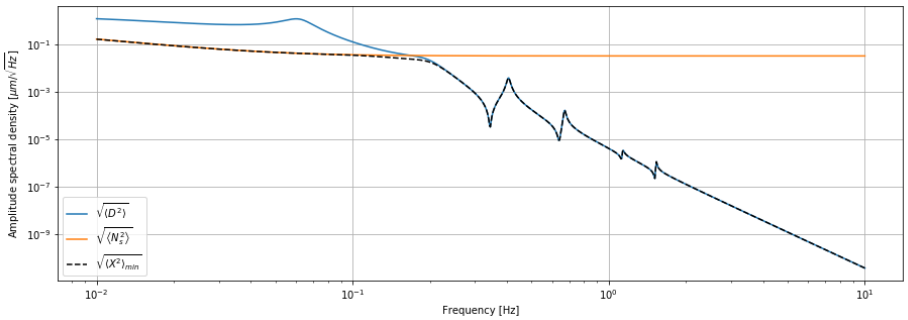

Figure 2: Amplitude spectral density of the external disturbance (blue solid line), sensor noise (yellow solid line) and the minimum residual motion (black dashed line).

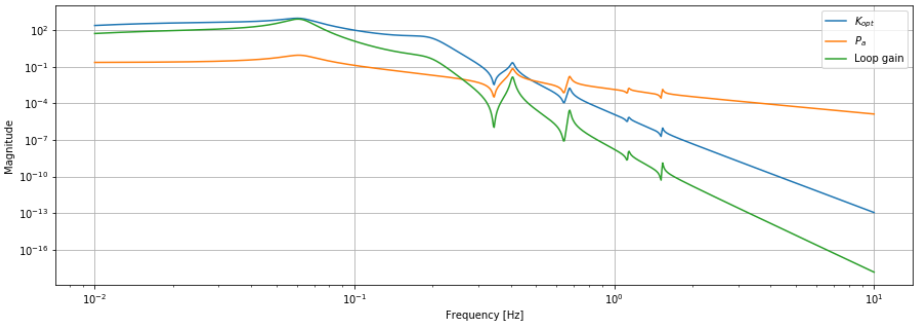

Figure 3: The controller Plant (yellow), theoretical optimal gain (blue) and the corresponding loop transfer function (green).

5 Optimal Controller

Here, we discuss some possible way to construct the optimal controller that is close to K_{opt}

5.1 H_∞/H_2 Optimal Controller

H_∞ and H_2 methods in control theory are ways to contrust robust controllers by minimization of the corresponding infinite and two norms. Ideally, a robust controller will achieve performance goals and stability within some bounded error in the system model. This feature is very important as long-term stability and guaranteed performance can both benefit long-term gravitational wave observation.

In contrast to block diagrams in classic control systems, a control process is modeled as a generalized plant in robust control methods such as H_∞ methods. The generalized plant P as shown in Fig. 4 has two inputs w and u,

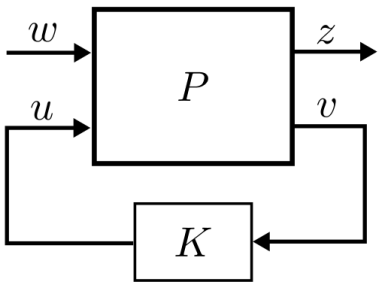

Figure 4: Generalized plant representation

and two outputs z and v. Also, the plant is stabilized by a controller K. Note that the generalized plant generally represents a MIMO system, meaning that the inputs and outputs are represented by vectors, whereas the plant and controller are matrices. In such configuration, the exogenous inputs w are all inputs including external disturbances and noise, error signals z are the quantities that have to be minimized, measured variables v are the measurements such as sensor signals which are used to calculate the manipulated variables u via the controller path K. In this representation, the open-loop input-output relationship is simply

$$\begin{pmatrix} z \\ v \end{pmatrix} = \begin{pmatrix} P_{11} & P_{12} \\ P_{21} & P_{22} \end{pmatrix} \begin{pmatrix} w \\ u \end{pmatrix}. \tag{12}$$

To determine the closed-loop behavior, the manipulated variables is set to $u = Kv$. Meanwhile, the input-output relationship becomes

$$z = G(P, K)\, w \tag{13}$$

where $G(P, K) = P_{11} + P_{12}K(I - P_{22}K)^{-1} P_{21}$ is the transfer function matrix relating the exogenous inputs to the error signals.[2] To approach H_∞ or H_2 optimal controllers, one has to formulate the controller design problem as a mathematical optimization problem, i.e. a cost function minimization problem. An H_∞ optimal controller has the cost function $||G(P, K)||_\infty$ minimized, whereas an H_2 optimal controller has the cost function $||G(P, K)||_2$ minimized. As can be seen, the purpose of an H_∞ or H_2 optimal controller conceptually is to minimize the impact of the external disturbances on the error signals hence exhibiting certain disturbance rejection and stabilization ability.

5.1.1 Interpretation of H_∞ and H_2 Norms

Minimizing the H norms is an alternative to approach the theoretical optimal controller K_{opt} in the form of Eqn. 6. Consider the control system of the preisolator as shown in Fig. 5. A corresponding generalized plant representation is shown in Fig. 6. Here, the external disturbance D and sensor noise N_s is represented by normalized noises $\hat{D}$

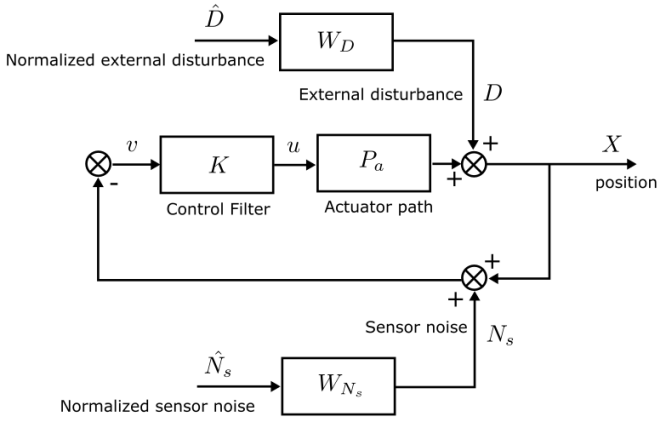

Figure 5: A modified block diagram of the preisolator with normalized disturbances and sensor noise as the external inputs.

and $\hat{N}_s$, i.e. Gaussian noise with magnitude of 1, which go through weighting functions W_D and W_{N_s} to become the original external inputs. Hence, the gain profile in the frequency response of the actual disturbances are represented by the weighting functions. This normalization is required since control methods, such as H_∞, H_2 and linear-quadratic-Gaussian control (LQG), assumes normalized inputs. With the weighting functions, one can better reflect the real disturbances in reality.

[2]The transfer function matrix $G(P, K)$ is often denoted $F_l(P, K)$ in control theory and mathematics. The reason why it has a special notation is because $F_l(P, K)$ is called the lower linear fractional transformation in mathematics

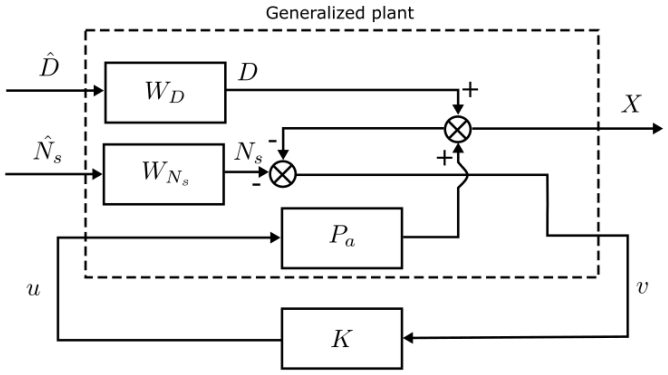

Figure 6: A generalized representation of the preisolator system

Using the generalized representation, the open-loop input-output relation is

$$\begin{aligned}\begin{pmatrix} z \\ v \end{pmatrix} &= P \begin{pmatrix} w \\ u \end{pmatrix} = \begin{pmatrix} P_{11} & P_{12} \\ P_{21} & P_{22} \end{pmatrix} \begin{pmatrix} w \\ u \end{pmatrix} \\ \left[\frac{X}{v}\right] &= \left[\begin{array}{cc|c} W_d & 0 & P_a \\ -W_d & -W_{N_s} & -P_a \end{array}\right] \left[\begin{array}{c} \hat{D} \\ \hat{N}_s \\ \hline u \end{array}\right],\end{aligned} \tag{14}$$

where the error signal is $z = X$ and the exogenous input is $w = \begin{pmatrix} \hat{D} \\ \hat{N}_s \end{pmatrix}$, v is the input to the controller while u is the output of the controller or the input to the actuation path. Meanwhile, the close-loop transfer function (CLTF) is

$$G = P_{11} + P_{12}K\left(I - P_{22}K\right)^{-1} P_{21} = \begin{pmatrix} \frac{W_D}{1+P_aK} & \frac{W_{Ns}P_aK}{1+P_aK} \end{pmatrix}. \tag{15}$$

Note that $z = Gw$ is identical to Eqn. 1 without the reference input.

H_2 Norm

From here, we can see that the H_2 norm of the CLTF is

$$\begin{aligned}||G||_2 &= \sqrt{\frac{1}{2\pi}\int_{-\infty}^{\infty} \mathrm{Tr}\left[G^{\mathrm{H}}G\right] d\omega} \\ &= \sqrt{\frac{1}{2\pi}\int_{-\infty}^{\infty} \left|\frac{W_D}{1+P_aK}\right|^2 + \left|\frac{W_{N_s}P_aK}{1+P_aK}\right|^2 d\omega},\end{aligned} \tag{16}$$

which happens be to the integrated RMS, i.e. the expected RMS, of the close-loop response $\mathbb{E}\left[\sqrt{\langle X^2\rangle}\right]$, if the weighting functions are scalar functions. Note that G^{H} is the conjugate transpose of G. As can be seen, an H_2 optimal controller K_{H_2} minimizes the expected value of $\langle X^2\rangle$, therefore as can be thought as a compromised version of K_{opt}, note that minimizing $\mathbb{E}\left[\sqrt{\langle X^2\rangle}\right]$ is the same as minimizing $\mathbb{E}\left[\langle X^2\rangle\right]$ itself.

H_∞ Norm

On the other hand, the H_∞ Norm of the CLTF is a much more interesting quantity. The H_∞ norm of the CLTF is defined as

$$||G||_\infty = \sup_{\omega\in\mathbb{R}} \bar{\sigma}\left(G\right), \tag{17}$$

where sup is the supremum and $\bar{\sigma}$ is the maximum singular value of G.

In MIMO systems, definitions of frequency response like magnitude and phase plots are not obvious. This is because the magnitude response of a MIMO system depends on the direction of the input w. Therefore, the magnitude responses at each particular frequency can be defined as the magnitude response of the CLTF for all possible inputs in the set $\{w \in \mathbb{C}^n\,;\, ||w||_2 = 1\}$. This magnitude response is also called the singular value denoted σ. Clearly, there exists an upper bound $\bar{\sigma}$ and lower bound $\underline{\sigma}$ for the singular value at each frequency and they respectively corresponds to the maximum and minimum of the square root of the eigenvalues $\lambda_i\left(G^H G\right)$.

At first glance, this might sound like a mathematical nonsense that has no physically significance. But, later we shall see that the minimizing the infinity norm of the CLTF is actually equivalent to minimizing the maximum residual motion $\left\langle X^2 \right\rangle$. Alternatively, the maximum singular value $\bar{\sigma}$ can be written as

$$\bar{\sigma}\left(G\right) = \max_{||w||_2=1} \sqrt{\sum_{i,j} \left|G_{ij} w_i\right|^2}. \tag{18}$$

Plugging in the transfer function matrix of the system, we get

$$\bar{\sigma}\left(G\right) = \max \sqrt{\left|\frac{W_D}{1+P_a K}\hat{D}\right|^2 + \left|\frac{W_{N_s} P_a K}{1+P_a K}\hat{N}_s\right|^2}, \tag{19}$$

under the condition

$$\left|\hat{D}\right|^2 + \left|\hat{N}_s\right|^2 = 1. \tag{20}$$

Subsequent maximization of $\sqrt{\sum_{i,j} \left|G_{ij} w_i\right|^2}$ at a particular frequency yields

$$\bar{\sigma}\left(G\right) = \begin{cases} \left|\frac{W_D}{1+P_a K}\right|, \text{if } \left|\frac{\mathrm{W_D}}{1+\mathrm{P_a K}}\right| > \left|\frac{\mathrm{W_{N_s} P_a K}}{1+\mathrm{P_a K}}\right| \\ \left|\frac{W_{N_s} P_a K}{1+P_a K}\right|, \text{if } \left|\frac{\mathrm{W_D}}{1+\mathrm{P_a K}}\right| < \left|\frac{\mathrm{W_{N_s} P_a K}}{1+\mathrm{P_a K}}\right| \end{cases}. \tag{21}$$

Recall that the weighting functions are defined such that $\left(W_D\right)\left(W_D\right)^H = \left\langle D^2 \right\rangle$ and $\left(W_{N_s}\right)\left(W_{N_s}\right)^H = \left\langle N_s^2 \right\rangle$, the square of singular value can be approximated as

$$\bar{\sigma}^2\left(G\right) \approx \begin{cases} \left|\frac{1}{1+P_a K}\right|^2 \left\langle D^2 \right\rangle, \text{if } \left|\frac{\mathrm{W_D}}{1+\mathrm{P_a K}}\right| > \left|\frac{\mathrm{W_{N_s} P_a K}}{1+\mathrm{P_a K}}\right| \\ \left|\frac{P_a K}{1+P_a K}\right|^2 \left\langle N_s^2 \right\rangle, \text{if } \left|\frac{\mathrm{W_D}}{1+\mathrm{P_a K}}\right| < \left|\frac{\mathrm{W_{N_s} P_a K}}{1+\mathrm{P_a K}}\right| \end{cases}. \tag{22}$$

Furthermore, it can be shown that $\bar{\sigma}^2\left(G\right)$ is approximately equal to $\left\langle X^2 \right\rangle$ if one of the disturbances dominates another. Therefore, minimizing $||G||_\infty$ can be seen as minimizing the supremum (across all frequencies) of the residual motion. And hence, can be thought as an alternative way of approaching K_{opt}.

Example 2

In this example, we compare the H_∞, H_2 and the theoretical optimal controller. The analysis is based on the previous example. Starting with Eqn. 14 as the generalized plant representation, we add one more quantity to the error signals such that $z = \begin{pmatrix} z1 \\ z2 \end{pmatrix} = \begin{pmatrix} X \\ W_u u \end{pmatrix}$, where W_u is a weighting function for bounding the manipulated variable. In this case, we set W_u to a relatively small number (10^{-6}) so Eqn. 14 is still effectively the plant to be controlled.

Under the same disturbances and sensor noise as the last example, H_∞ and H_2 optimal controllers were synthesized using the "hinfsyn" and "h2syn" function from the python control library. The frequency responses of the controllers and the loop transfer functions are shown in Fig. 7. Judging from the stability margins, both controllers have guaranteed stability as robust control techniques are meant to synthesize very stable controllers. Another important feature to note is that both synthesizing techniques yield controllers which has an $1/P_a$ component in the gain profile just like K_{opt} in Eqn. 6.

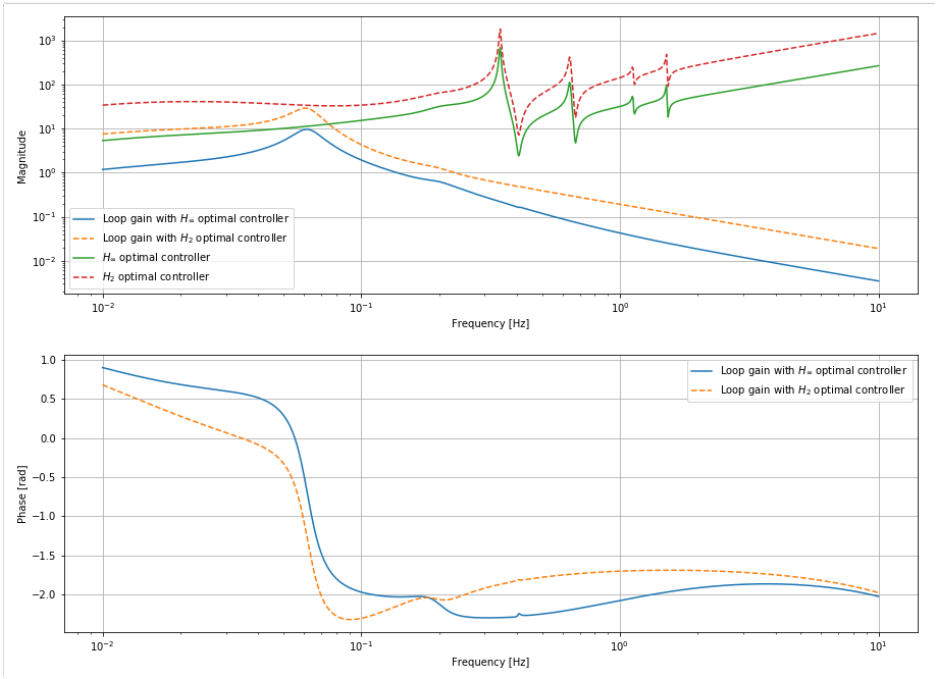

Figure 7: Frequency responses of the H_∞ (green solid line) and H_2 (red dotted line) optimal controllers and the corresponding loop transfer functions (blue solid line and yellow dotted line).

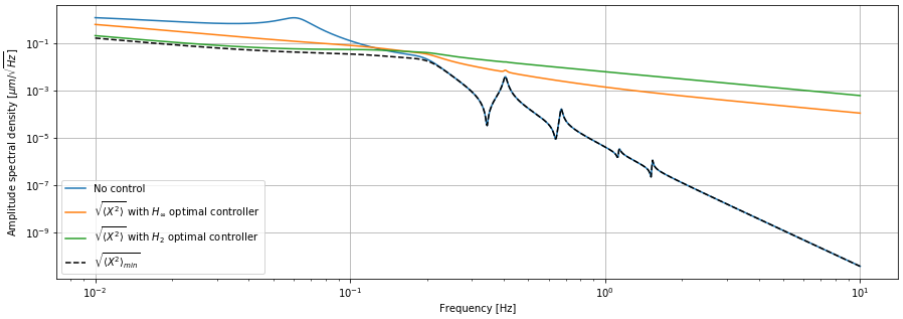

Figure 8: Amplitude spectral density of the residual motion corresponding to no control (blue solid line), H_∞ optimal controller (yellow solid line), H_2 optimal control (green solid line) and the theoretical optimal controller (black dashed line).

As can be seen from the amplitude spectral density plot Fig. 8, both H_∞ and H_2 controllers can greatly suppress the seismic noise induced resonance at around 0.7 Hz (1-order reduction). However, noise attenuation is not great compare at higher frequencies. If noise attenuation is required at higher frequencies, a high-pass weighting function can be used for the displacement error signal to penalize high frequency residual motion. Such method corresponds to the mixed sensitivity problem (see next section).

5.2 Mixed Sensitivity Controller

As we can see from the last section, a pure H_∞/H_2 optimal controller is able to suppress distinctive disturbances at particular frequencies but can unfavorable at other frequencies. In particular, from Fig. 8, we can see that there is large difference between the H_∞/H_2 optimal residual motion and the minimum residual motion at high frequencies. This can be a problem as high frequency noise will directly compromise the sensitivity of the gravitational wave detector. In this case, one will need some way to specify performance goals to the control problem such that a stabilizing controller can be synthesized with guaranteed performances. The method of mixed sensitivity allows weightings to be assigned to the error signals, effectively changing the cost function of the optimization problem. Moreover,the weightings can be frequency depending, meaning that one would be able to specify frequency dependent targets for the error signals as well as deciding the control bandwidth, etc.

To use mixed sensitivity methods, the generalized plant representation has to be slightly modified. The new plant is called an augmented plant where frequency dependent weights are used to calculate the error signals. The augmented version of Fig. 6 is shown in Fig. 9. Under this configuration, the weighting functions W_X and W_u can be set such

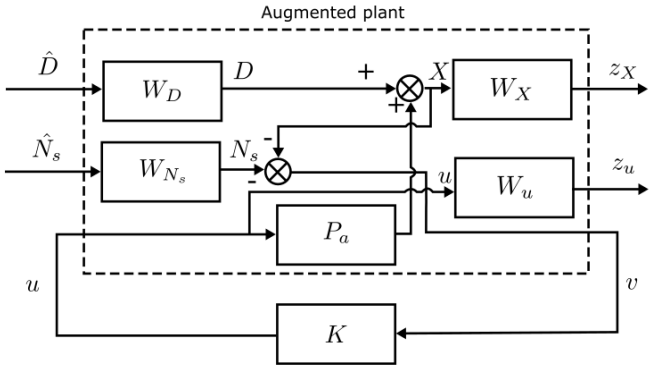

Figure 9: Augmented plant for the preisolator with weighted manipulated variables and weighted displacement as the error signals

that they are the reciprocals of the targeted outputs. This is the case, because $\hat{D}$ and $\hat{N}_s$ are normalized. In the previous example, W_u was set to 10^{-6}. This corresponds to setting an upper limit for the manipulated variable at 10^6 at all frequencies. In this manner, if we know the residual motion requirement, the weighting function W_X can be simply be set to the inverse of that such that the algorithm can synthesis the controller according to the requirements.

An important note for robust control systems in general, is that setting requirements does not guarantee such targets to be met. Synthesizing a robust controller can be thought as searching a filter in a pool of stable controllers such that a cost function is minimized. It is possible that there exists no controllers in the set which can satisfy all conflicting requirements. In other words, by setting weighting functions, we can tip the trade-off between robustness and performance. But, there is always a physical limit. So one has to design the weighting functions carefully in order to make ensure the existence of such optimal filter.

Example 3

To demonstrate the ability of mixed sensitivity methods, we introduce weighting functions W_X to example 2 according to Fig. 9 such that $z = \begin{pmatrix} z1 \\ z2 \end{pmatrix} = \begin{pmatrix} W_X X \\ W_u u \end{pmatrix}$. We keep $W_u = 10^-6$ and set W_X according to the gain profile in Fig. 10.

The gain of the displacement weight is around 10 below 0.1 Hz and gradually increases to 10^5 above 10 Hz. This corresponds to setting the displacement requirement to 0.1 $\mu m/\sqrt{Hz}$ at low frequency and 10^{-5} $\mu m/\sqrt{Hz}$ at above 10 Hz. As can be seen from Fig. 11, the displacement levels at 10 Hz are reduced to $< 10^{-6}$ $\mu m/\sqrt{Hz}$ for both H_∞ and H_2 controller (10^{-4} $\mu m/\sqrt{Hz}$ and 10^{-3} $\mu m/\sqrt{Hz}$ in Fig. 8). However, suppression at lower frequencies has

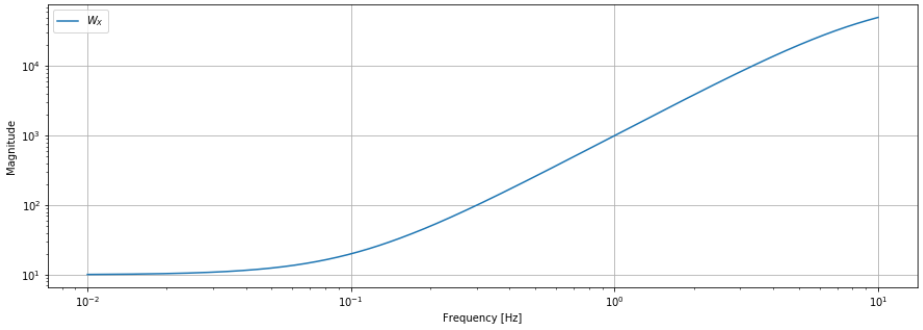

Figure 10: Gain profile of the weighting function of the displacement

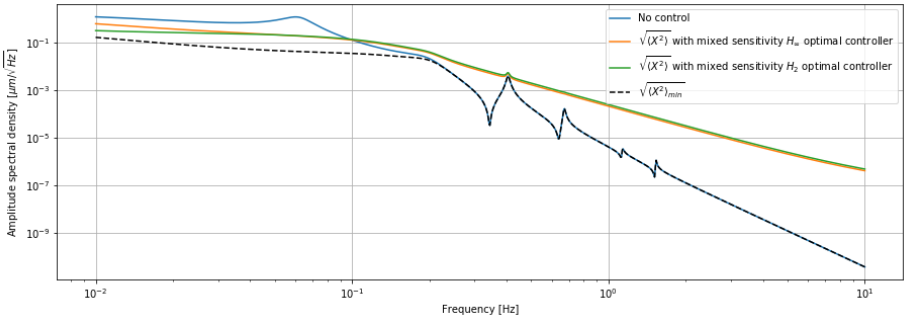

Figure 11: Residual motion according to no control (blue solid line), mixed sensitivity H_∞ optimal controller (yellow solid line), mixed sensitivity H_2 optimal controller (green solid line) and the theoretical optimal controller (black dashed line).

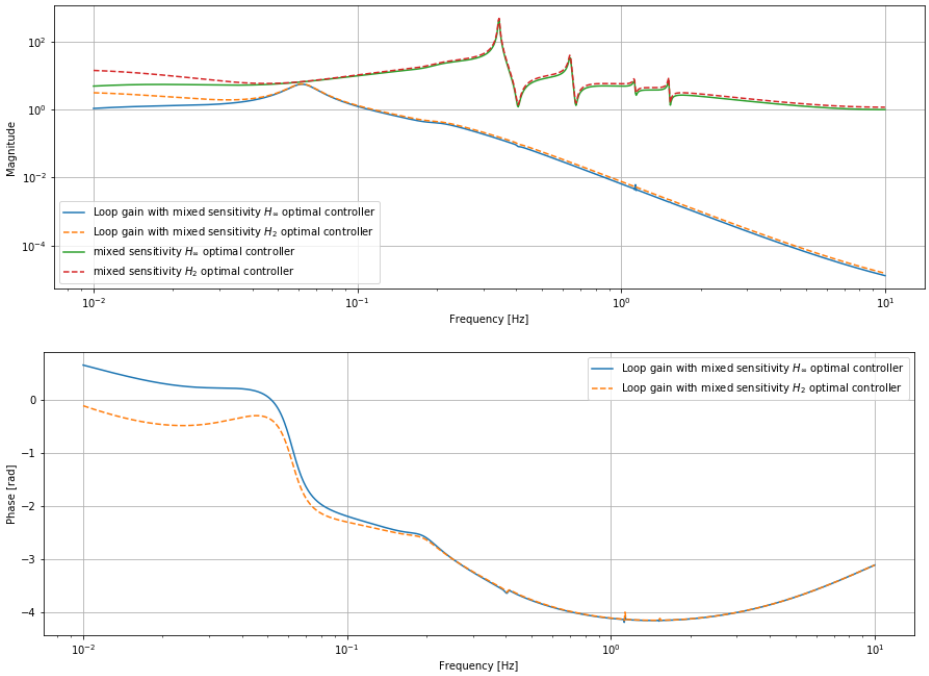

Figure 12: Frequency responses of the mixed sensitivity H_∞/H_2 (green solid/red dashed) optimal controller and the corresponding loop transfer functions (blue solid/yellow dashed).

reduced as a compromise.[3]

[3]This phenomenon is referred to the famous waterbed effect in control problems. The waterbed effect is a result from the Bode's sensitivity integral where if a system has suppressed disturbances at some frequencies, it is necessarily increased in other frequencies.

5.3 Comment on Weighting Functions

As shown in the examples, the optimal controllers were synthesized according to the weighting functions that simulate input spectral densities as well as weighting functions that specify the performance requirement. Therefore, the key to having a truly optimal controller is to properly shape the weighting functions such that they lead to the true optimal control law. This can be difficult at times because some noise spectra simply cannot be approximated by gain profile of transfer functions. A proper way to design weighting functions is yet to be determined. A possible way to design weight functions would be to utilize the integrated RMS of the disturbances and noises as well as the crossover of the spectrums. Another possibility would be to iteratively do mathematical optimization of predetermined weighting functions such that the simulated residual motion is minimized.

6 Adaptive Control

6.1 Necessity

With the robust control synthesis techniques in last section, it is possible to construct control filters that can provide optimal seismic disturbance rejection. But, this is true for a certain period of time only. As can be seen from Miyo-san's record of the seasonal change of the seismic noise in KAGRA [4], the seismic noise changed drastically in terms of both magnitude and frequency dependency. In Fig. 13, two "nominal" seismic noise spectrum S1 and S2 are

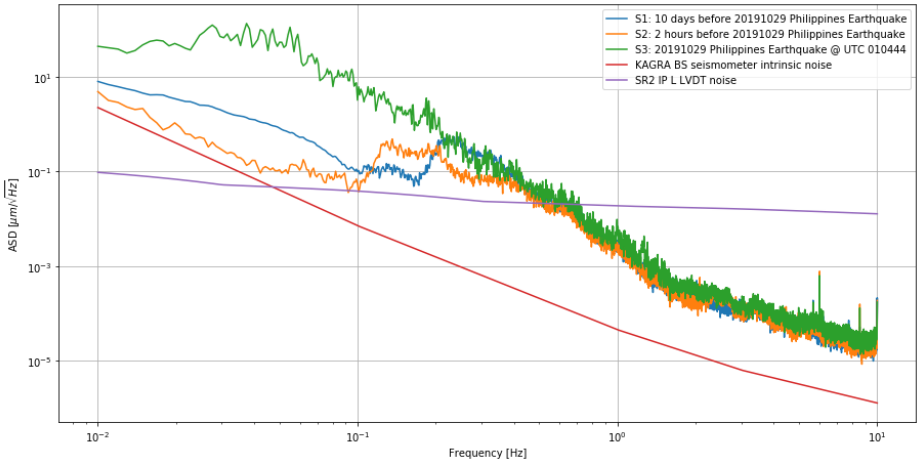

Figure 13: Comparison between three noise spectrum measured by the seismometer near the BS in KAGRA. S1: 10 days before 20191029 Philippines earthquake (blue), S2: 2 hours before 20191029 Philippines earthquake (yellow), S3: Philippines earthquake (green). The actual seismomter self-noise (red) of the seismomter and SR2 inverted pendulum sensor noise (cyan) are plotted for reference.

shown along with a spectrum S3 taken during the Philippines 6.6 magnitude earthquake which happened on the 29$^{\text{th}}$ October, 2019. S1 and S2 are approximately 10 days apart and S2 was taken 2 hours before S3.

Comparing S1 and S2, a drastic increase in displacement level at low frequencies can be observed. Moreover, the micro-seismic peak also varied from 0.2 Hz to between 0.1 Hz and 0.2 Hz. As can be seen in Fig. 14 the optimal loop gains suppressing S1 and S2 would carry drastically different magnitude with different control bandwidth. Additionally, a tremendous increase in low frequency loop gain is required for suppressing the disturbances in the event of an earthquake.

According to Eqn. 11, having a high enough loop gain can constrain the displacement level close to the sensor noise, which is very close to optimal. So, one would argue that having a high enough loop gain at low frequency could easily suppress all level of seismic noise. But, regardless of the inability of actuators, this would set a sensitivity

[4] Available here: https://github.com/MiyoKouseki/kagra-gif/issues/108.

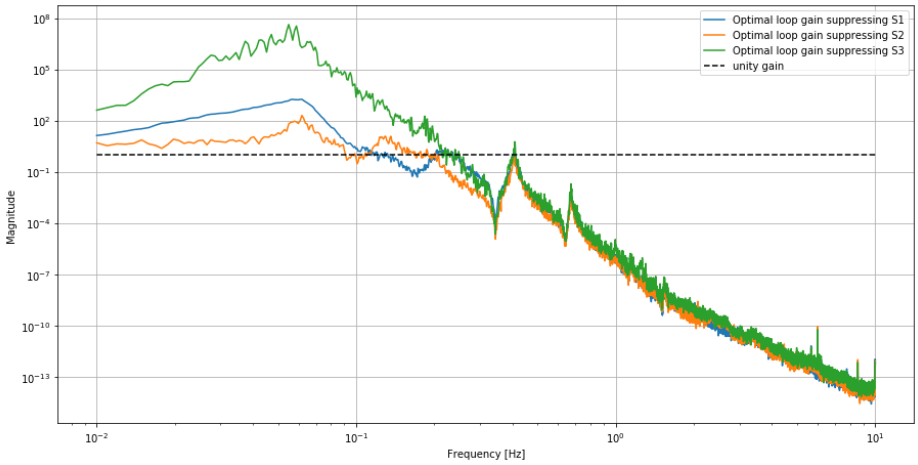

Figure 14: Theoretical optimal loop gain for suppressing S1 (blue), S2 (yellow) and S3 (green) as shown in Fig. 13.

limit at higher frequencies because of the waterbed effect as mentioned in example 3. Therefore, it is important to realize an optimal loop gain that is high enough at low frequency and low enough at high frequency to give extra sensitivity margin during observation mode, while not compromising the robustness of the control system. The solution to this problem is given by the robust methods as discussed in the last section. But, since the disturbance changed drastically with time, it would require the controller to be continuously updated according to the real-time disturbance.

6.2 Concept

6.2.1 Self-tuning Adaptive Robust Control.

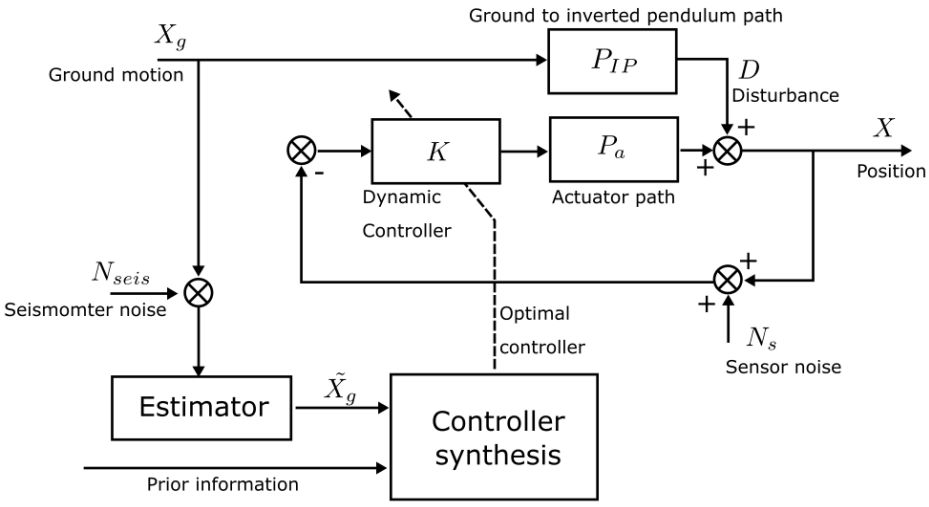

Figure 15: Pre-lock acquisition local self-tuning adaptive robust control system

Fig. 15 shows the proposed adaptive control scheme for pre-lock aquisition local control [5]. Here, we adopt the simple feedback loop as described in Fig. 1. The disturbance D to the preisolator platform position is the preisolator filtered

[5]The proposed adaptive control scheme should be ideally a model identification adaptive control scheme, where the controller synthesis process should take into account also the measured position. However, because there is no way to measure the sensor noise, the measured displacement is degenerated and it would be difficult to identify only the contribution from the ground motion. Therefore, we propose to use prior knowledge of the sensor noise to reconstruct the actual position.

ground motion $P_{IP}X_g$, where X_g is the ground motion and P_{IP} is the ground to preisolator transfer function. The ground motion is sensed by a seismometer with self-noise N_{seis} which is placed near the suspension. From the seismometer signal, we would be able to estimate the real-time seismic noise. Combined with prior information of the suspension plants P_{IP}, P_a, and the sensor noise N_s, it is possible to estimate the new weighting functions W_D and W_{N_s} which are part of the augmented plant/generalized plant reflecting the real parameters in real-time. With the updated plant, we can proceed to synthesize a new optimal control according to the methods in section 5, or other loop-shaping methods if necessary, and update the controller parameters accordingly. These procedures can be done periodically with a programmatic loop. So, in this way, the controller can be automatically tuned such that it is always optimal.

Example 4

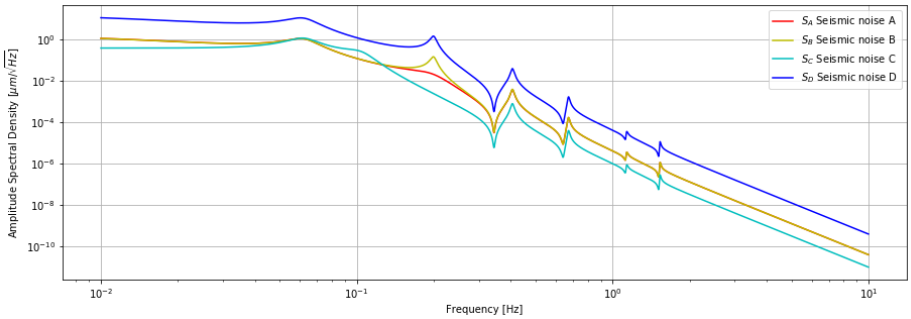

Figure 16: 4 disturbance spectrum representing some possible types of variation in the seismic noise. S_A: Nominal (red), S_B: Increase in micro-seismic activity at 0.2 Hz (yellow), S_C: Shifted micro-seismic peak from 0.2 Hz to 0.1 Hz (cyan) and S_D: A broadband increase in seismic level according to S_B (blue).

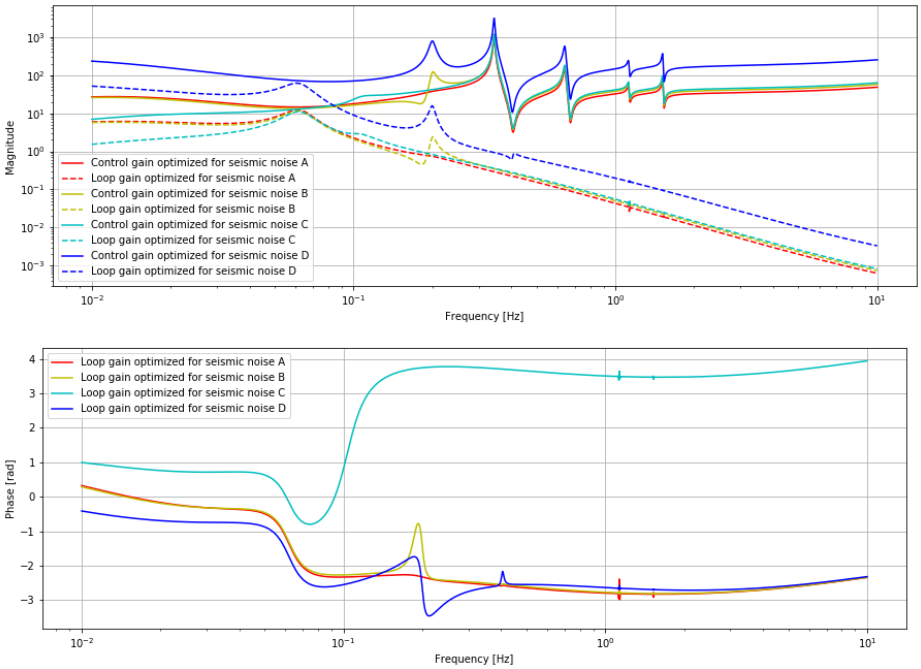

Figure 17: Frequency response of the control gains and loop gains optiimzed for the four disturbances spectrum

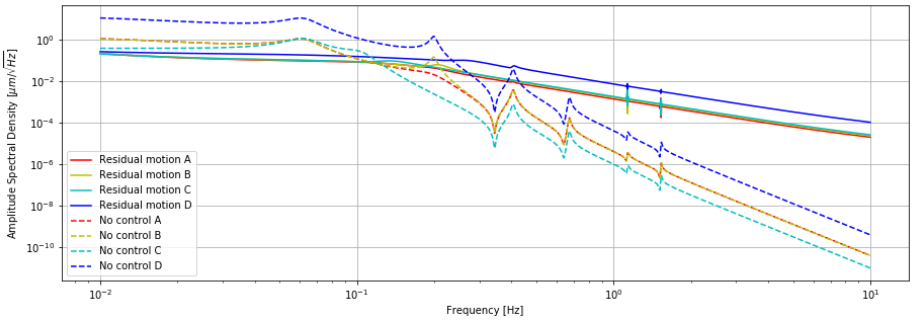

Figure 18: Comparison between of the damped and undamped residual motion in all four scenarios described in Fig. 16. Solid lines are the residual motions when the corresponding optimal controller is engaged and dashed lines are the uncontrolled residual motions.

In Fig. 16, four possible variations of the seismic noise is demonstrated, namely (S_A, S_B, S_C and S_D, four seismic disturbance scenarios.). We followed section 5.2 to design four different H_2 optimal controllers as if the self-tuning process is in action. Fig. 17 shows the corresponding optimal controllers for suppressing the four noises. As can be seen, in all four optimal controllers, additional control gain at high disturbances region is given. This means that the controller can reacts to the new disturbances and suppress correspondingly. And, as shown in the residual plot Fig. 18, all external disturbances are attenuated accordingly, with the cost of slight increase of high frequency noise. This demonstrate the power of such adaptive control scheme.

In fact, in example 4, the constraints posed by weights in while optimizing controller for suppressing S_C was so tight, that it over-constrained the problem so that plant is actually unstable and actually there is no solution in the H_∞ sense. The idea can be traced back to eqaulity where $S + T = 1$ and that S and T cannot be simultaneously minimized. And in fact, if we slightly modify the output weighting function W_X and loosen the restrictions, the algorithm can generate a plant that is stable and has some suppression ability (See Fig. 19 and Fig. 20 for the Bode plot of the revamped S_C controller and performance.).

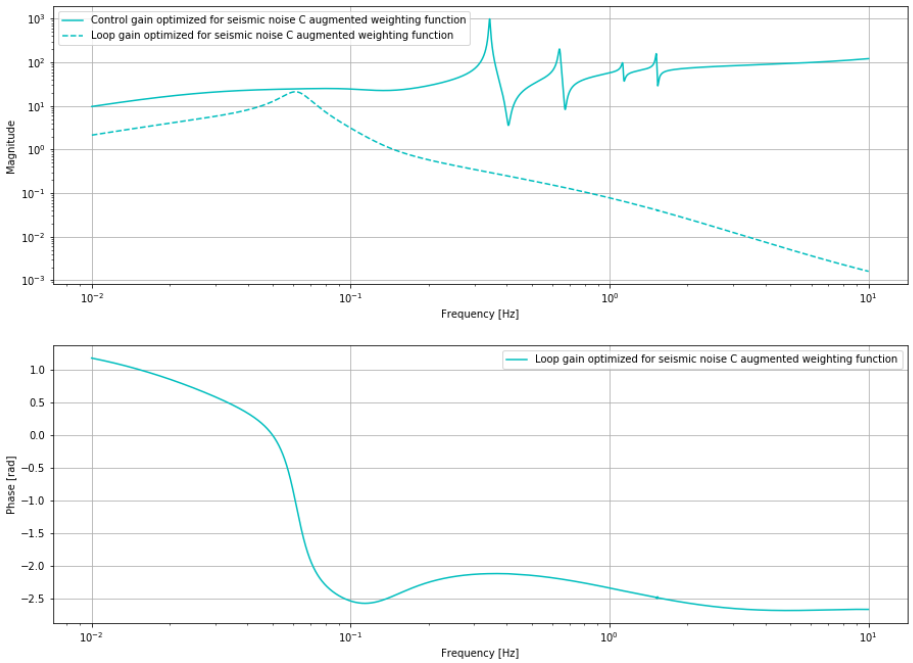

Figure 19: Bode plot of the stabilizing controller for seismic noise C with a modified output weighting function.

To further emphasize the importance of an adaptive approach, the residual motion is plotted again but with a static controller that is optimized for suppressing S_A in Fig. 16. As shown in Fig. 21, the static controller cannot handle the drastic changes in the seismic noise and those changed additive disturbance will be transmitted to the residual

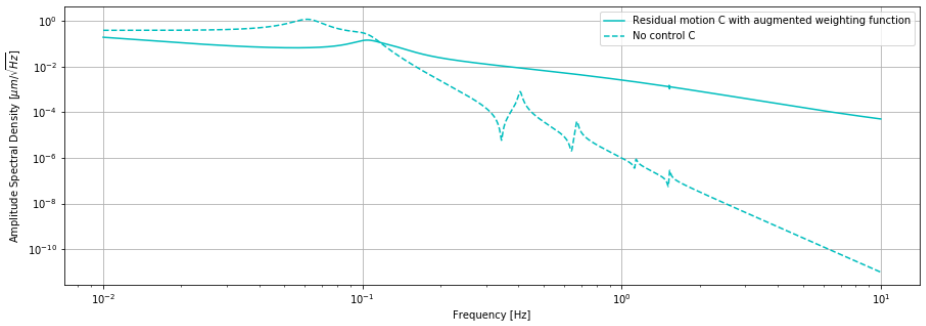

Figure 20: Ampltitude spectral density comparision between damped and undamped with the new controller optimized for suppressing S_C

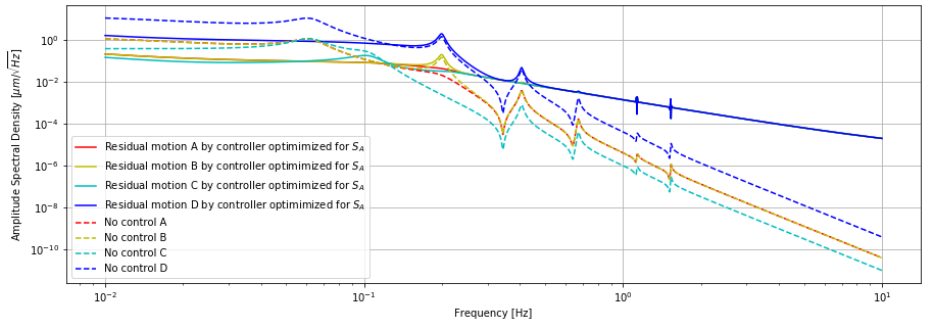

Figure 21: Residual motion in all four scenarios but using a static controller optmized for seismic noise A (red in Fig. 16.

motion of the system.

6.3 Limitations

Optimization Window and Delay

Ideally, the controller should be updated between every cycle of the digital system so all controller outputs are truly always optimal. However, this would require the controller synthesis process to be completed within one control cycle which is likely to be unrealistic. Also, instead of real-time data, we can only use measured data to compute new controllers. This means that the new controller is only optimal with respect to past data but not exactly optimal at the present and for the the short period in the future. So, the controller will be sub-optimal if the rate of change of the seismic noise level is fast relative to update rate of the adaptive control.

But, it might be able to get away with this limitation if sudden perturbations, such as earthquakes, is not considered. Luckily, the seasonal change of the seismic noise is very slow so it can be assumed to be quasi-static. In comparison, the controller optimization process of took a few seconds in my computer. Moreover, even if there is a slight variation in the seismic noise level during the synthesis, the older controller should be able to deal with it because robust controllers are meant to handle slight variations and uncertainty in a system.

To mitigate the effect of sudden ground perturbations, the system should be further equiped with a feedforward filter that actively cancels the seismic noise. For example, an adaptive least-mean-square feedforward filter can be used to remove high SNR ground pertubations, see section 7.

(The following paragraph may be ignored because we need high gain at low frequency for position control anyway and that the ground signal SNR is high at micro-seismic)

Low Signal-to-Noise Ratio

One limitation of this approach would be the low SNR $\frac{\langle X_g^2 \rangle}{\langle N_{seis}^2 \rangle}$ at low frequencies. Since inertial sensors like seismometers are intrinsically AC-coupled, the seismometer noise N_{seis} at low frequencies is very high, see Fig. 13 for reference. Therefore, it would be undesirable to use the unprocessed seismometer signal to esitimate the external disturbances to the preisolator, unless the low frequency noise performance can be improved. Therefore, to estimate a proper disturbance level which can be used for synthesizing an optimal controller that does not exceedingly introduce low frequency noise, we must design a weighing function (filter) that attenuates low SNR signals during the estimation.

6.4 Automatic Optimization of the Weighting Functions

As can be seen from previous examples, mixed sensitivity H_∞/H_2 optimal control synthesis is a very useful tool for designing optimal controllers. Combined with adaptive control, we can formulate a dynamic stable robust controller that can react to drastic changes in the plant while maximizing possible noise performance. Ultimately, this will provide great improvement in terms of the stability of the interferometer and will make lock-acquisition easier with the presence of high environmental disturbances.

From the previous examples, it is easy to see that weight functions play important roles during the synthesis. In H_∞/H_2 optimal sense, the controller is only optimal according to the cost function, which is indirectly defined by the weighting functions. So, with ill-designed weights, the generated controller can easily produce adverse closed-loop performance, such as instability and poor attenuation. Therefore, we need some way to design the weight functions such that it gives a controller that 1) is closed-loop stable and 2) gives the best performance possible.

There is really no standard way of choosing such weighting functions and this is still an ongoing problem in control theory. In [1], they presented an optimization approach using genetic algorithms (GA) and structured genetic algorithms (sGA) to find, not just the coefficients defining the weightings, but also the order of the functions. Such ability is very desirable for our purpose because there is really no way to predetermine the best order that is required for the weighting functions. This is especially important for identifying the seismic noise weighting function because the predetermined functional form might not be able to capture all seismic noise that we can see.

To achieve proper weighting function designs (or even the controller itself), we can rely on global optimizer such as GA and sGA as demonstrated in [1]. Because it is possible to evaluate a controller's actual performance (i.e. by simulation), we can present the performance in a fitness or cost function and then optimize the parameters of the weightings so that the controller synthesis process really gives the best controller with respect to the reality. In this sense, the controller synthesis process is not an simply a one-time process but should be an iterative process while the weightings or parameters are being optimized with respect to the measured disturbance.

One might fear that such global optimization approaches might drastically increase the time that is used for synthesizing the optimal controller. But, there is always some way that can make optimization process faster. Using GA as an example, indeed, there is a limitation on how quick the optimization process can be. This is because the algorithm starts with a completely randomized population of candidates and so the optimization might take long for the candidates to evolve from something entirely not optimal. So, this might reduce the effectiveness of the adaptive control due to excessive delay.

Here, we briefly discuss two ways that we can evade from this problem. One way is to have an genetic algorithm running continuously but will return the best candidate of the latest generation which can be used to update the controller. Once a new measurement is available, we update the cost function inside the ongoing genetic algorithm so eventually it will gradually give better controllers on each return. In this case we can evade the long time that is needed for evolution. Another approach would be to planting a seed in the initial pool of randomized candidates so the randomized candidates can learn from the seed so the result should converge much quicker. In this case the seed would be the previous controller.

6.4.1 Weightings on Weightings

In the MathWorks example of a mixed sensitivity design of an active car suspension [6], the suspension deflection weighting function and acceleration weighting function are each multiplied by a relative weighting β and $1-\beta$. And, by having different values of β, different controllers can be constructed for different driving modes such as comfort, balanced and handling.

In the same manner, we can have output weighting functions which corresponds to disturbance rejection and noise attenuation and have relative weightings on them. Before lock-acquisition, high disturbance rejection is required so we set higher priority for disturbance rejction and low priority for noise attenuation. During the observation, noise performance at high frequency is desirable so we can set relative weighting on noise rejection to be high. In this way, we can define different operation modes for the suspension to accommodate various needs from the interferometer.

7 Adaptive Filters

Not to be confused with adaptive control, adaptive filtering is the idea of having an adjustable filter that is self-corrected to minimize some error signals, while adaptive control is a big set of approaches that deal with uncertainties and time-varying parameters in a control plant. Well known usages of adaptive filter are system identification and noise cancellation, which can be found in MathWorks [7] This is a very useful and easy-to-implement tool but is simply absent in daily KAGRA works. Here, we will briefly discuss the possibility of using adaptive filters as feedforward filters (sensor correction, seismometer feedforward, length to angle cancellation filter) and as a system identification tool (possibly an adaptive one.).

7.1 Sensor Correction

Throughout the analysis in previous chapters, we assume that the sensor correction is perfect and that the measurement signal is perfectly seismic noise-free. However, in reality, the sensor correction is only close to perfect at higher frequencies (> 0.1 Hz). This is because we typically assume that the seismometer noise is much higher than seismic noise at lower frequencies therefore the correction filter is designed to be a high-pass filter with very steep roll-off at around 0.1 Hz so to not introduce additional sensor noise at low frequency. However, this is an obstruction to the optimal control topology because the control bandwidth is in some sense limited by the sensor correction filter. As can been seen from Fig. 14, the optimal gain is actually dominated at frequencies lower than 0.1 Hz, as in, seismic noise is most problematic at those frequencies. But, if sensor correction is not implemented at those frequencies, the controller would be introducing seismic noise (as a sensor noise) instead of providing suppression. And, since there exists high gain at low frequencies for position control anyway, the sensor correction should be done adaptively to remove noises from the relative sensors at frequencies where seismic noise is dominated (i.e. seismic noise higher than seismometer noise).

Fig. 22 shows an adaptive noise cancellation scheme using adaptive algorithms such as least means square algorithm. In the figure, s is the signal contaminated by some measurement noise n and n_0 is some noise correlated to the measurement noise n. The error signal e is the summation of the measurement and a filtered noise $\hat{n}$ which is also correlated to n, i.e.

$$e = s + n - \hat{n}. \tag{23}$$

The square of the error signal is

$$e^2 = s^2 + (n-\hat{n})^2 + 2s\,(n-\hat{n})\,. \tag{24}$$

And, it follows that minimizing the mean of the squared error signal gives

$$\min \mathbb{E}\left[e^2\right] = \mathbb{E}\left[s^2\right] + \min \mathbb{E}\left[(n-\hat{n})^2\right], \tag{25}$$

[6] Available here: https://www.mathworks.com/help/robust/gs/active-suspension-control-design.html.
[7] Available here https://www.mathworks.com/help/dsp/ug/overview-of-adaptive-filters-and-applications.html.

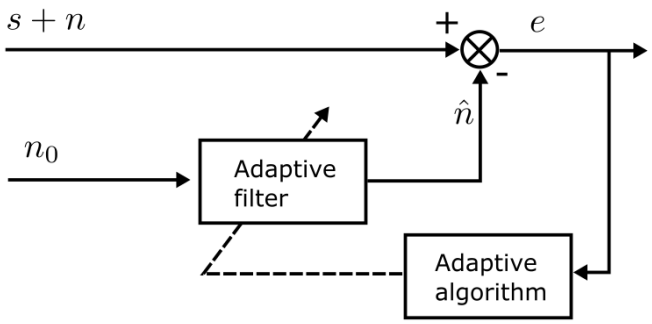

Figure 22: Noise cancellation using apadative filter

given that the signal s is uncorrelated with the noise n_0. From Eqn. 25, we can see that minimizing the mean squaure of the error signal is equivalent to minimizing the power of the noise. Therefore, to achieve noise cancellation, an adaptive algorithm can be used to automatically find coefficients of the adaptive filter such that the mean of the error squared is minimized. Least mean square and recursive least square are some well-established algorithms that can achieve the minimization of mean squared quantities and so they can be readily implemented.

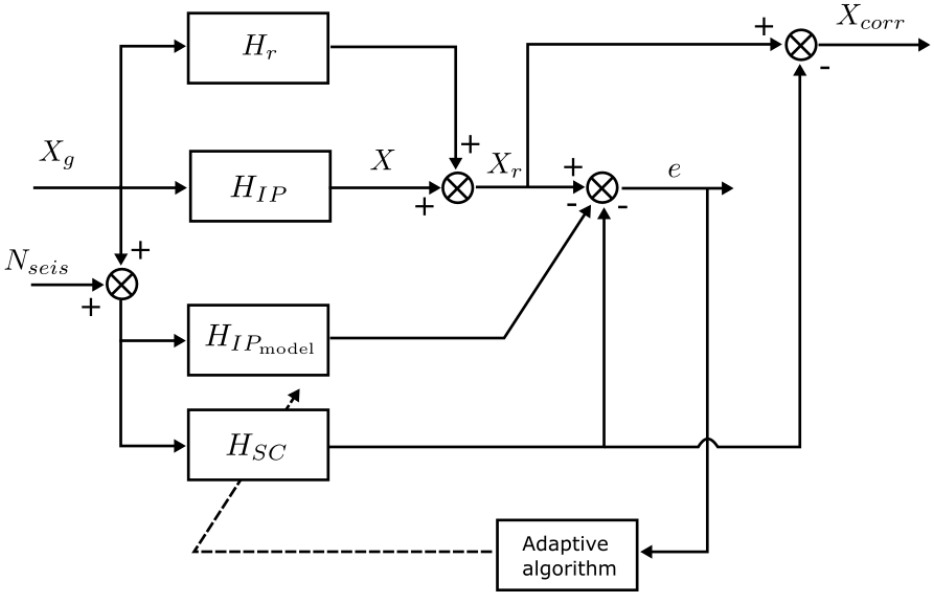

Figure 23: Adaptive sensor correction configuration.

For sensor correction purposes, the diagram in Fig. 22 has to be modified slightly to Fig. 23. This is because the desired sensor output is the response of the preisolator, which is also correlated to the seismic noise. In Fig. 23, X_g is the seismic noise, X is the actual displacement of the preisolator platform, X_r is the displacement sensed by the relative displacement sensor (LVDT) and X_{corr} is the sensor corrected displacement. The relative displacement reads $X_r = X_g H_{IP} + X_g H_r$, where H_{IP} is the closed-loop response of the inverted pendulum and H_r is the coupling from the ground to the relative sensor. In the ideal case, the sensor correction filter H_{SC} should cancel out the effect of the coupling H_r from the relative sensor such that the corrected signal X_{corr} is exactly equal to the displacement of the preisolator platform X. Using the noise cancellation approach as described in Fig. 22, a seismometer with self-noise N_{seis} can be used to actively cancel the ground coupling from the relative sensor. However, this cannot be done without an extra path $H_{IP_{\text{model}}}$, the modeled response, which preserves the inverted pendulum response because we don't want to cancel it from the sensing readout. Under this configuration, the error signal reads

$$e = X_g H_{IP} + X_g H_r - (X_g + N_{seis})\,(H_{IP_{\text{model}}} + H_{SC})\,. \tag{26}$$

Assuming that the modeled response is idential to the actual response, then the error signal simplies to

$$e = X_g \left(H_r - H_{SC}\right) + N_{seis} \left(H_{IP_{\text{model}}} + H_{SC}\right). \tag{27}$$

Consequently, the least mean square error becomes

$$\min \mathbb{E}\left[e^2\right] = \min \mathbb{E}\left[X_g^2 \left(H_r - H_{SC}\right)^2\right] + \min \mathbb{E}\left[N_{seis}^2 \left(H_{IP_{\text{model}}} + H_{SC}\right)^2\right]. \tag{28}$$

Under the least mean square condition, it is easy to see that the sensor correction filter converges to two values at two extremes,

$$H_{SC} = \begin{cases} H_r \,,\; X_g^2 \gg N_{seis}^2 \\ -H_{IP_{\text{model}}} \,,\; N_{seis}^2 \gg X_g^2 \end{cases}. \tag{29}$$

Then, the corrected signal is

$$X_{corr} = X_g H_{IP} + X_g H_r - \left(X_g + N_{seis}\right) H_{SC} = \begin{cases} X_g H_{IP} \,,\; X_g^2 \gg N_{seis}^2 \\ N_{seis} H_{IP_{\text{model}}} \,,\; N_{seis}^2 \gg X_g^2 \end{cases}. \tag{30}$$

Recall that $H_{IP_{\text{model}}}$ is proportional to the sensitivity function $\frac{1}{1+P_a K}$ which is effectively a high pass filter, the seismometer noise N_{seis} will be attenuated from the corrected signal X_{corr} at lower frequencies where $N_{seis}^2 \gg X_g^2$ happens, whereas, the term $X_g H_r$ will be canceled when the seismic noise dominates. Under such adaptive correction scheme, the sensor correction filter will be automatically tuned to allow active damping at frequencies where seismic noise dominates.

7.2 Feedforward and the Like (and Cancellation Filters like, Length to Angle decoupling, in General))

The least mean square adaptive filter in Fig. 22 is very generic and can be applied to cancellation filters for seismometer feedforward as well as frequency depending decoupling filters between varies degrees of freedom such as length to angle cancellation filters. In particular, the frequency depending decoupling filter can sometimes be problematic as high precision of modeling is needed and a slight change in the system can easily ruin the effectiveness of cancellation. So, instead of a static approach, the filter should be set also adaptively to cancel out such cross-couplings. Fig. 24 shows the adaptive cancellation approach. We will not discuss this matter thoroughly as the mathematics is basically the same as previously described. One important thing to note is that this approach can be used as system identification even if we choose not to use an adaptive approach. One can simply inject actuation signal in direction A and let the adaptive algorithm to automatically minimize the error signal. Once the adaptive filter has converged, it can be simply recorded and used as a static cancellation filter. This gives a much more accurate cancellation filter as opposed to that of manual transfer function fitting.

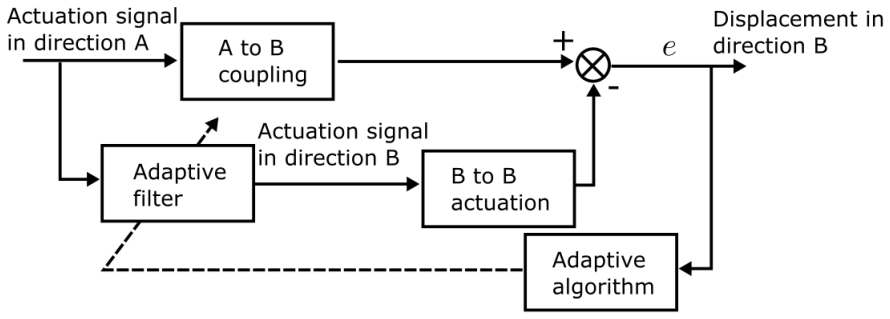

Figure 24: Adaptive filter for cancellation of frequency depending cross-coupling between two degrees of freedom A and B.

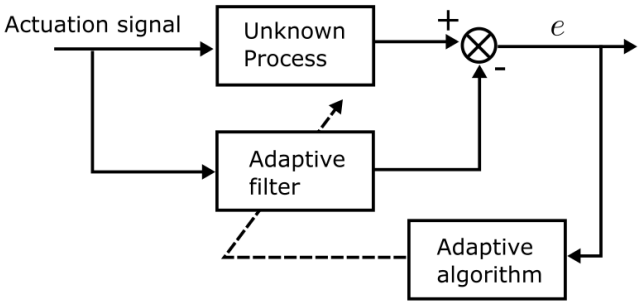

Figure 25: System identification using adaptive filter

7.3 System Identification using (also) Adaptive Filters

In previous sections, modeled plants are frequently used. For example, the actuation plant P_a is used for controller synthesis. It is important that we model the a system accurately so to facilitate further optimization. Therefore, we propose to use adaptive filters to accurately model a system. Fig. 25 shows the same least mean square adaptive filter as previously shown. If we set up the signals this way, it follow that the adaptive filter will be identical to the unknown plant as the error signal is minimized. In such a way we can model a system automatically. Furthermore, oftentimes we will know the number of coefficients that are needed to describe a particular plant. In this sense, we can predetermine the functional form of the adaptive filter to enhance the accuracy of modeling.

8 Implementation Plan

9 Machine Learning reinforced Adaptive Control

10 Generalization

References

[1] Eva Alfaro Cid, Euan McGookin, and David Murray-Smith. Optimisation of the weighting functions of an h_∞ controller using genetic algorithms and structured genetic algorithms. *International Journal of Systems Science*, 39:335–347, 04 2008.